



EVALUATION OF CFSR CLIMATE DATA FOR HYDROLOGIC PREDICTION IN DATA-SCARCE WATERSHEDS: AN APPLICATION IN THE BLUE NILE RIVER BASIN¹

Yihun Taddele Dile and Raghavan Srinivasan²

ABSTRACT: Data scarcity has been a huge problem in modeling the water resources of the Upper Blue Nile basin, Ethiopia. Satellite data and different statistical methods have been used to improve the quality of conventional meteorological data. This study assesses the applicability of the National Centers for Environmental Prediction's Climate Forecast System Reanalysis (CFSR) climate data in modeling the hydrology of the region. The Soil and Water Assessment Tool was set up to compare the performance of CFSR weather with that of conventional weather in simulating observed streamflow at four river gauging stations in the Lake Tana basin — the upper part of the Upper Blue Nile basin. The conventional weather simulation performed satisfactorily (e.g., $NSE \geq 0.5$) for three gauging stations, while the CFSR weather simulation performed satisfactorily for two. The simulations with CFSR and conventional weather yielded minor differences in the water balance components in all but one watershed, where the CFSR weather simulation gave much higher average annual rainfall, resulting in higher water balance components. Both weather simulations gave similar annual crop yields in the four administrative zones. Overall the simulation with the conventional weather performed better than the CFSR weather. However, in data-scarce regions such as remote parts of the Upper Blue Nile basin, CFSR weather could be a valuable option for hydrological predictions where conventional gauges are not available.

(KEY TERMS: hydrologic cycle; time series analysis; meteorology; CFSR; SWAT; Ethiopia; Upper Blue Nile basin; Lake Tana basin.)

Dile, Yihun Taddele and Raghavan Srinivasan, 2014. Evaluation of CFSR Climate Data for Hydrologic Prediction in Data-Scarce Watersheds: An Application in the Blue Nile River Basin. *Journal of the American Water Resources Association* (JAWRA) 1-16. DOI: 10.1111/jawr.12182

INTRODUCTION

Several hydrological modeling studies have been carried out in the Upper Blue Nile basin, Ethiopia. Some of these studies (e.g., Liu *et al.*, 2008; Uhlenbrook *et al.*, 2010; Gebrehiwot *et al.*, 2011) have sought to understand the hydrology of the region,

while others (e.g., Abdo *et al.*, 2009; Beyene *et al.*, 2009; Elshamy *et al.*, 2009; Kim and Kaluarachchi, 2009; Betrie *et al.*, 2011; Setegn *et al.*, 2011; Taye *et al.*, 2011) have applied hydrological models to assess the implications of environmental and management changes on the water resources in the region. Hydrological modeling has been used to inform the teleconnection between upstream and

¹Paper No. JAWRA-13-0074-P of the *Journal of the American Water Resources Association* (JAWRA). Received March 22, 2013; accepted January 3, 2014. © 2014 American Water Resources Association. **Discussions are open until 6 months from print publication.**

²Ph.D. Candidate (Dile), Stockholm Resilience Center, Stockholm University, Kräftriket 2B, 106 91, Stockholm, Sweden and Stockholm Environment Institute, Linnégatan 87D, 104 51 Stockholm, Sweden; and Professor (Srinivasan), Spatial Sciences Laboratory in the Department of Ecosystem Sciences and Management, Texas A&M University, 1500 Research Parkway, College Station, Texas 77845 (E-Mail/Dile: yihun.dile@sei-international.org).

downstream countries (e.g., Barrett, 1994; Conway and Mike, 1996).

These modeling efforts have ranged from simple conceptual models (e.g., Kim and Kaluarachchi, 2008; Liu *et al.*, 2008; Conway, 2009; Uhlenbrook *et al.*, 2010) to complex, physically based distributed hydrological models (e.g., Mishra and Hata, 2006; Setegn *et al.*, 2010; White *et al.*, 2011). However, these modeling efforts have not always gone smoothly. One of the main challenges they have faced has been the limited availability of hydrometeorological data (Kim and Kaluarachchi, 2008; Kim *et al.*, 2008; Collick *et al.*, 2009; Mekonnen *et al.*, 2009; Melesse *et al.*, 2010). Improved data collection and management is needed to increase the reliability of hydrological modeling efforts in the Upper Blue Nile basin.

Many studies have explored ways to improve the quality of hydro-climatic data in the Upper Blue Nile basin. Some (e.g., Barrett, 1994; Tsintikidis *et al.*, 1999; Ymeti, 2007) have applied satellite data as inputs to hydrological models. Others have employed various statistical methods to fill data gaps (e.g., Betrie *et al.*, 2011; Tesemma *et al.*, 2009; Uhlenbrook *et al.*, 2010) or to generate finer-resolution inputs from coarser datasets (e.g., Engida and Esteves, 2011). Tsintikidis *et al.* (1999) applied daily average aerial precipitation from METEOSAT satellite data to study the sensitivity of the Blue Nile region's hydrologic response to the type of precipitation data (i.e., rain gauge-based *vs.* satellite-based estimates). Similarly, Barrett (1994) utilized METEOSAT satellite inputs to predict the inflows into the Aswan High Dam and to forecast flow hydrographs at selected gauging locations above the dam. Ymeti (2007) estimated rainfall from geostationary METEOSTAT Second Generation (infrared channel) and orbiting Tropical Rainfall Measurement Mission (TRMM; microwave channel) satellite data and assessed the performance of two conceptual rainfall-runoff models. Tesemma *et al.* (2009) and Uhlenbrook *et al.* (2010) used regression and spatial interpolation to fill data gaps. Most of the studies that have applied the Soil and Water Assessment Tool (SWAT) (e.g., Betrie *et al.*, 2011) have used a daily weather generator (WXGEN) (Neitsch *et al.*, 2012) to generate climatic data or to fill gaps in measured records. While these are some of the various efforts exerted to improve hydro-climatic data quality in the Upper Blue Nile basin, global reanalysis data sources are becoming very promising options in representing observed weather data (*cf.*, Zhang *et al.*, 2012).

Global reanalysis weather data have been used for various hydrological applications all over the world and yielded sound results (Lavers *et al.*, 2012; Najafi *et al.*, 2012; Fuka *et al.*, 2013; Quadro *et al.*, 2013; Smith and Kummerow, 2013; Wei *et al.*, 2013). For

example, Smith and Kummerow (2013) analyzed the surface and atmospheric water budgets of the Upper Colorado River basin using reanalysis, *in situ*, and satellite-derived datasets. The reanalysis data they used included National Aeronautics and Space Administration Modern-Era Retrospective Analysis for Research Applications (MERRA), the European Centre for Medium-Range Weather Forecasts (ECMWF) interim Reanalysis (ERA-Interim), and the National Centers for Environmental Prediction's Climate Forecast System Reanalysis (CFSR). They found that all datasets captured the seasonal cycle for each water budget component. Likewise, Najafi *et al.* (2012) generated reasonable volumetric estimates of the streamflow of the snow-dominated East River basin, a tributary of the Gunnison River in the Colorado River basin, with the Sacramento Soil Moisture Accounting (SAC-SMA) model using CFSR data. Fuka *et al.* (2013) used CFSR precipitation and temperature data in modeling five small watersheds representing different hydroclimates (four in the United States and one in Ethiopia) in SWAT. Their findings suggest that utilizing CFSR precipitation and temperature data for watershed models can predict the streamflow as good as or better than simulations using traditionally observed weather data. Lavers *et al.* (2012) used five atmospheric reanalysis products — CFSR, ERA-Interim, 20th Century Reanalysis (20CR), MERRA, and NCEP-NCAR (National Center for Atmospheric Research) — to detect atmospheric rivers (narrow plumes of enhanced moisture transport in the lower troposphere) and their links to British winter floods and large-scale climatic circulation. Their study provided valuable evidence of generally good agreement on atmospheric river occurrences between the products. Quadro *et al.* (2013) evaluated the hydrological cycle over South America using CFSR, MERRA, and the NCEP Reanalysis II (NCEP-2). They observed general agreement in precipitation patterns among the three products and the observed precipitation over much of South America. They reported that the CFSR precipitation showed the smallest biases. Wei *et al.* (2013) used the CFSR dataset to study the water budgets of three tropical cyclones that passed through the Taiwan Strait. They assessed the quality of CFSR for tropical cyclone studies by comparing CFSR precipitation data with TRMM precipitation data. They concluded that the CFSR data were reliable for studying tropical cyclones in this area.

The applicability of global reanalysis climate data for hydrological model predictions in the Upper Blue Nile basin has not so far been adequately investigated. The present study, focusing on a relatively data-rich part of the basin, assesses the applicability of CFSR data for hydrological predictions.

MATERIALS AND METHODS

Study Area

The research presented in this article was carried out in the Lake Tana basin, in the upper reaches of the Upper Blue Nile basin, Ethiopia. The Lake Tana basin is located in northwestern Ethiopia (latitude 10.95° to 12.78°N, and longitude 36.89° to 38.25°E) and has a drainage area of approximately 15,000 km² (MoWR, 1998) (Figure 1). The Lake Tana basin falls inside four administrative zones (Figure 1). Agaw Awi and West Gojjam cover the southern part, South Gondor the eastern part, and North Gondor the northern part. The climate of the basin is dominated by tropical highland monsoon with most of the rain (~70-90%) occurring between June and September (Mohamed *et al.*, 2005; Conway and Schipper, 2011). The major rivers feeding Lake Tana are the Gilgel Abay, the Rib, the Gumara, and the Megech (Figure 1).

Hydrologic Model

The applicability of global weather data for hydrological modeling in data-scarce regions was tested using the 2012 version of the SWAT model (SWAT2012). SWAT is a physically based model, developed to predict the impact of land-management practices on water, sediment, and agricultural chemi-

cal yields in watersheds with varying soil, land use, and management conditions (Neitsch *et al.*, 2012). SWAT can simulate hydrological cycles, vegetation growth, and nutrient cycling with a daily time step by disaggregating a river basin into subbasins and hydrologic response units (HRUs). HRUs are lumped land areas within the subbasin comprised of unique land cover, soil, and management combinations. This allows the model to reflect differences in evapotranspiration and other hydrologic conditions for different land cover and soil (Neitsch *et al.*, 2012). SWAT has been applied in the highlands of Ethiopia and demonstrated satisfactory results (Easton *et al.*, 2010; Setegn *et al.*, 2010; Betrie *et al.*, 2011). The SWAT model requires spatial, temporal, and management data to model the hydrology of a watershed.

Spatial Data

The spatial data used in SWAT for the present study included digital elevation model (DEM) data, stream network data, and soil and land cover data. The DEM data were required to delineate the watersheds in the ArcSWAT interface. The stream network data were required to superimpose onto the DEM data to define the location of the streams. The soil and land cover data were important to define the HRUs. The Shuttle Radar Topographic Mission DEM dataset was obtained from the CGIAR Consortium for Spatial Information website (CGIAR-CSI, 2009), and has a resolution of 90 m × 90 m. The stream

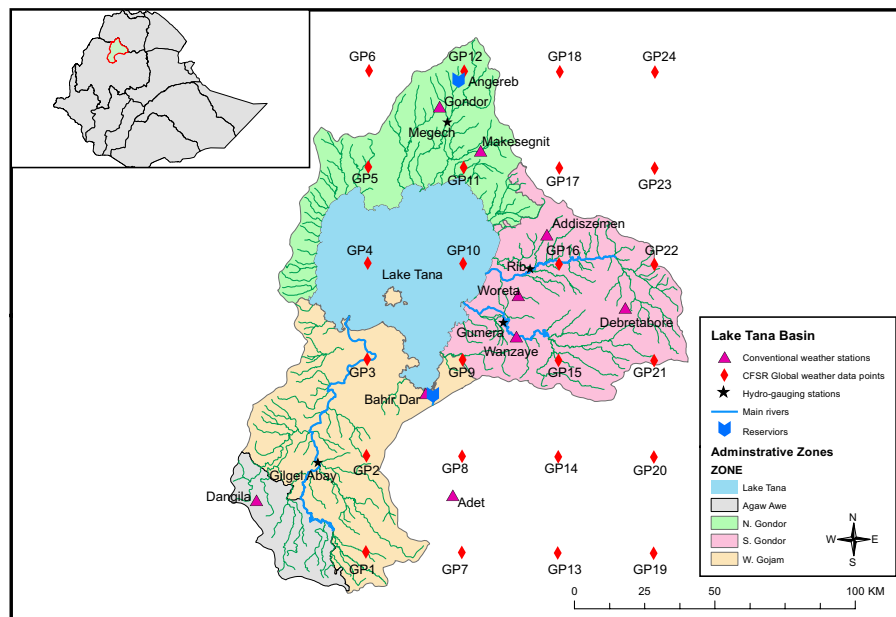


FIGURE 1. Map Showing the Lake Tana Basin in the Ethiopian River Basin System, Including Hydrometeorological Stations and Administrative Zones.

network, land use, and soil maps of the study area were collected from the Ethiopian Ministry of Water Resources (MoWR, 2009). The soils' physical and chemical properties parameters required by SWAT were derived from the digital soil map of the world CD-ROM Africa map sheet (FAO, 1995).

A large part (~75%) of the Lake Tana basin is under cultivation (Table 1). The two agricultural land use types in the original land use system (i.e., dominantly cultivated and moderately cultivated) were reclassified into TEFF and CORN SWAT land use codes. Teff and corn are the most widely cultivated crop types in Ethiopia (EIAR, 2007; CSA, 2012). The water body (i.e., the lake) is the second largest type of land cover in the basin.

There are 10 identified soil types in the Lake Tana basin. A large part of the soil has loam and clay-loam soil texture. The different soil types and their hydrological characteristics are presented in Table 2.

Hydrometeorological Data

Weather data are used to simulate the hydrological processes in SWAT. It is difficult to obtain high-quality weather data for the Upper Blue Nile basin. The main objective of this study was to investigate options that could replace the available observation

data, or data sources in data-scarce regions for hydrological modeling purposes. We applied two types of weather data in raw SWAT simulations (i.e., simulations without calibration). The two weather data sources used were observed weather data from climatic stations in and around the Lake Tana basin (hereafter called "conventional weather") and weather data from the NCEP's CFSR (hereafter called "CFSR weather") (Saha *et al.*, 2010).

The conventional weather has daily rainfall, and maximum and minimum temperature from nine climatic stations (Figure 1). It spans the period 1990-2011. The highest (1,575 mm) and the lowest (927 mm) average annual rainfalls in the period from 1990-2010 occurred at Dangila and Makesnit weather stations respectively. Dangila is located in the south of the Lake Tana basin, and Makesnit in the north.

The conventional weather has many data gaps (Table 3). Most of the gaps are in the data for 1990-1993, a period of political upheavals in Ethiopia. SWAT's built-in weather generator was used to fill data gaps in the conventional weather (Neitsch *et al.*, 2012). The weather station data in SWAT can be linked to the subbasins using the centroid method (Neitsch *et al.*, 2012) and time-dynamic Voronoi tessellation method (Andersson *et al.*, 2012). In this study, we used the centroid method. The conventional weather was collected from the Ethiopian National Meteorological Services Agency (ENMSA, 2012).

The CFSR weather was obtained for a bounding box of latitude 10.95°-12.78°N and longitude 36.89°-38.25°E (the Texas A&M University spatial sciences website, globalweather.tamu.edu) (Globalweather, 2012). It includes rainfall, maximum and minimum temperature, wind speed, relative humidity, and solar radiation for 24 locations (Figure 1). The CFSR weather is produced using cutting-edge data-assimilation techniques (both conventional meteorological

TABLE 1. Dominant Land Cover Classes in the Lake Tana Basin.

Land Cover Types	Area (% of basin)
Dominantly cultivated	51.35
Moderately cultivated	22.34
Water body	20.19
Woodland, open; shrubland; Afro-alpine; forest	2.91
Grassland	2.83

Note: Plantations, swamp, and urban areas cover less than 1% of the basin.

TABLE 2. Major Soil Types in the Lake Tana Basin with Their Physical and Hydrological Characteristics for the Top Layer.

FAO Soil Name	Area (% of basin)	Texture	Moist Bulk Density (g/cm ³)	Saturated Hydraulic Conductivity (mm/hr)	Available Water Holding Capacity (mm H ₂ O/mm soil)
Haplic Luvisols	20.62	Loam	1.4	5.95	0.106
Chromic Luvisols	16.00	Clay-Loam	1.4	4.37	0.148
Eutric Leptosols	12.38	Loam	1.2	14.53	0.063
Eutric Vertisols	11.74	Clay	1.2	13.89	0.1
Eutric Fluvisols	9.79	Loam	0.9	64.74	0.175
Haplic Alisols	4.77	Clay	1.1	23.32	0.164
Lithic Leptosols	2.86	Clay-Loam	1.3	7.11	0.094
Haplic Nitisols	1.29	Clay-Loam	0.8	88.4	0.166
Eutric Regosols	0.28	Sandy-Loam	1.4	21.25	0.15
Eutric Cambisols	0.01	Loam	1.1	23.61	0.167

Notes: FAO, Food and Agriculture Organization of the United Nations.

Water bodies (representing 20.3% of the basin) and urban (less than 1% of the basin) land use types have unidentified soil types.

TABLE 3. Rainfall Information (1990-2010) for the Conventional Weather and CFSR Weather in the Lake Tana Basin.

Station Name	Average Annual Rainfall (mm/year)	Percentage of Missing	Elevation (m.a.s.l)
Addizemen	1219.6	9.6	1940
Adet	1125.4	19.0	2080
Bahir Dar	1419.4	2.1	1790
Dangila	1575.2	3.7	2120
Debretabore	1502	9.6	2690
Gondor	1145.3	5.2	1967
Makesegnit	927	1.6	1912
Wanzaye	1377.1	7.0	1821
Woreta	1168.5	10.1	1819
GP1	1843	NA	2362
GP2	800.6	NA	2068
GP3	403.5	NA	1811
GP4	407.5	NA	1784
GP5	1796	NA	1836
GP6	2402	NA	1531
GP7	1692.9	NA	2730
GP8	510	NA	2169
GP9	548.9	NA	1833
GP10	772.1	NA	1784
GP11	1048.5	NA	1794
GP12	1674	NA	2417
GP13	1388.7	NA	2109
GP14	800.6	NA	2247
GP15	1212.8	NA	2054
GP16	1302.3	NA	1815
GP17	718	NA	2031
GP18	1045.7	NA	2032
GP19	484.4	NA	2023
GP20	468.8	NA	2399
GP21	1398	NA	2783
GP22	1204.5	NA	2784
GP23	262.3	NA	1742
GP24	345.2	NA	1841

Note: NA, no missing data observed.

gauge observations and satellite irradiances) as well as highly advanced (and coupled) atmospheric, oceanic, and surface-modeling components at ~38 km resolution (Saha *et al.*, 2010). This indicates that the production of CFSR data involves various spatial and temporal interpolations (on the presented conventional weather data in Table 3, other nearby conventional observations, and satellite products). It is uncertain whether this process would yield similar climatic results to the conventional weather, which is one reason for this comparative study.

According to the CFSR weather, the highest and lowest annual rainfalls in 1990-2010 were 2,402 and 262.3 mm. These occurred at weather stations GP6 and GP23 (Figure 1), respectively. Both weather stations are located in the northern part of the Lake Tana basin, but outside the basin boundary. The CFSR weather does not have any data gaps. Table 3 compares the conventional weather and the CFSR weather using annual rainfall.

The performance of the conventional and CFSR weather for simulating streamflow were evaluated using the streamflow data at gauging stations in four rivers in the Lake Tana basin: the Gilgel Abay, the Gumera, the Rib, and the Megech. The Gilgel Abay (catchment area 5,004 km²) is the largest tributary, draining into Lake Tana from the southern part of the basin. The Gumera (catchment area 1,893 km²) and the Rib (catchment area 2,464 km²) flow into Lake Tana from the east. The Megech (catchment area 2,620 km²) flows in from the north. The gauged parts of the Gilgel Abay, Gumera, Rib, and Megech are 2,025, 1,595, 1,407, and 514 km² and the elevation ranges from the lake at 1,876 m.a.s.l to 2,795, 2,915, 3,400, and 2,890 m.a.s.l for the Gilgel Abay, Gumera, Rib, and Megech, respectively. The hydrological data span the period 1990-2007 and were supplied by the Ethiopian Ministry of Water and Energy (MoWE, 2012). This limited our evaluation of the model simulation to 1990-2007, even though climate data were available up to 2010. As the purpose of the study was to compare the performance of CFSR weather simulation in relation to conventional weather simulation, we did not perform any model calibration.

The Lake Tana elevation-area-volume curve from Wale *et al.* (2009) and Angereb reservoir data from the municipal water supply authority for Gondor town (GWSA, 2012) were used as input for the reservoirs in SWAT. Daily lake outflows from the Lake Tana reservoir in 1990-2007 and average monthly reservoir outflows from Angereb were used for reservoir simulations. The average amount of water drawn from the Angereb reservoir for consumption was considered in the reservoir simulation. Table 4 presents physical reservoir parameter inputs for the model.

Model Setup

The watersheds were delineated to achieve a stream network compatible with the stream network provided from the Ministry of Water Resources (MoWR, 2009). SWAT is a hydrological model and its performance is improved with homogeneous subbasin sizes. Hence, the sizes of the subbasins were fixed between 500 and 3,000 ha. Multiple HRUs were created within each subbasin, and zero percent threshold area was used to define HRUs (i.e., all land use, soil, and slope classes in a subbasin were considered in creating the HRUs). Water bodies along the stream network were considered as reservoirs in the SWAT model. Hence, the natural Lake Tana and the artificial Angereb reservoir created to supply water to Gondor were both included as reservoirs in the model. Data on agricultural management practices in the basin were obtained from the Ethiopian Institute of Agricultural Research

TABLE 4. Physical Parameters of Reservoirs in the Lake Tana Basin.

	Principal Spillway			Emergency Spillway		
	Elevation (m.a.s.l)	Area (km ²)	Volume (Mm ³)	Elevation	Area (km ²)	Volume (Mm ³)
Lake Tana	1,784	2,766	20,300	1,787	2,983	29,100
Angereb reservoir	2,135	0.5	3.53	2,138	0.6	5.16

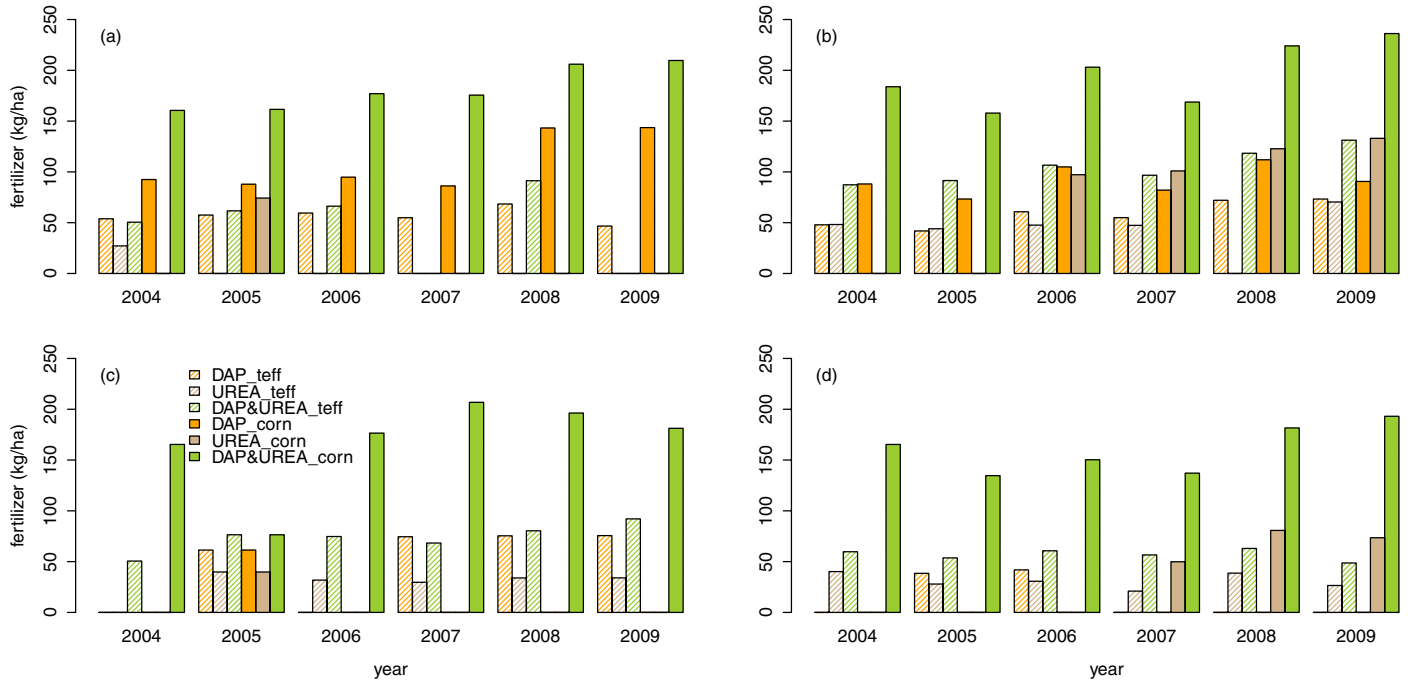


FIGURE 2. Different Fertilizer Application Practices in Four Administrative Zones in the Lake Tana Basin: (a) Agew Awi, (b) West Gojjam, (c) South Gondor, and (d) North Gondor.

(EIAR, 2007) and the Ethiopian Central Statistical Agency (CSA, 2012). Management practices data included planting, harvesting and killing, tillage, and fertilizer and pesticide applications.

The timing of planting and harvesting in the study area varies from year to year based on the onset of the rainy season. In this study, the timing of harvesting and planting was averaged over a longer period. Thus, for the purpose of the simulations, teff was planted on July 22 and harvested on December 5, and corn was planted on May 20 and harvested on October 25.

Tillage distributes nutrients, pesticide, and residue in the soil profile. A traditional tilling tool called the *maresha* is used in Ethiopia. The depth of tillage with the *maresha* ranges from 15 to 20 cm (Gebregziabher *et al.*, 2006; Temesgen *et al.*, 2008). Tillage frequency generally varies depending on the situation of a particular farmer, the location, the crop, and climatic factors (Temesgen *et al.*, 2008). In setting up this model, a tillage frequency of four times per year, to a depth of 15 cm, and a mixing efficiency of 0.3 was implemented (Temesgen *et al.*, 2008).

The blanket recommendation for fertilizer application in most parts of Ethiopia is 100 kg DAP per ha plus 100 kg UREA per ha (EIAR, 2007). DAP is a phosphorous-based fertilizer with the composition 45.5-46.5% phosphate (P_2O_5), 17.5-18.3% nitrogen, 1.5-2.6% water, and 2-4% fluoride. UREA is a 46% nitrogen fertilizer. EIAR (2007) recommends application of 100 kg/ha of DAP at one application, along with 50 kg/ha UREA applied at planting, and another 50 kg/ha applied after 30 to 35 days.

In practice, fertilizer application in the study area does not always follow these recommendations. Data on various fertilizer application practices from 2004-2009 were obtained from the Central Statistical Agency (CSA, 2012). They are summarized in Figure 2. In Ethiopia, fertilizer application data are available only at the level of administrative zones. Fertilizer application practices differ among the administrative zones, and also within the zones (i.e., it differs from farmer to farmer). The farmers apply either DAP or UREA, or a combination. However, for this study we used the best-case fertilizer application

practice (combined DAP and UREA application) in the respective zones, but averaged over years.

The EIAR (2007) recommends the application of 2,4-D Amine weedkiller to protect crops from weed damage 7 to 10 weeks after planting. As per the EIAR's recommendation, 2,4-D Amine weedkiller was added at 1 l/ha on teff fields in the model setup. This weedkiller was not applied on cornfields, as it is not recommended for broad-leafed crops.

SWAT has different options to calculate the hydrological components in a watershed. In this study, the Hargreaves method was used to determine potential evapotranspiration, since it only required air temperature data. Surface runoff was estimated using the Soil Conservation Service's curve number method, which is a nonlinear function of precipitation and retention coefficients. The surface runoff in SWAT is estimated separately for each HRU and routed to obtain the total runoff for the watershed. A variable storage routing method was used for routing the flow of water in the channels. As the aim of this study was to assess the applicability of global data for hydrological applications, model calibration was not performed. Calibrations are necessary to improve the model performance for a given climatic input.

Model Evaluation

The model was simulated from 1990-2011, with a three-year warm-up period to let all hydrological stocks balance from their initial state. The performance of the model was evaluated at four river gauging stations using Nash-Sutcliffe Efficiency (NSE) and Percent bias (PBIAS).

Nash-Sutcliffe Efficiency is a normalized statistic that determines the relative magnitude of the residual variance compared to the measured data variance (Nash and Sutcliffe, 1970). It is calculated with Equation (1).

$$\text{NSE} = 1 - \frac{\sum_{i=1}^n (Q_{\text{obs}}^i - Q_{\text{sim}}^i)^2}{\sum_{i=1}^n (Q_{\text{obs}}^i - Q_{\text{obs}}^{\text{mean}})^2} \quad (1)$$

where Q_{obs}^i and Q_{sim}^i are the observed and simulated streamflow at the i th time step respectively; $Q_{\text{obs}}^{\text{mean}}$ is the average of the observed streamflow; and n is the total number of observations. NSE values can range from $-\infty$ to 1. An NSE value of 1 corresponds to a perfect match of observed streamflow to simulated streamflow. An NSE value between 0 and 1 is considered an acceptable level of performance, whereas an NSE value ≤ 0 suggests the observed average is a better predictor than the model.

Percent bias compares the average tendency of the simulated data to the corresponding observed data (Gupta *et al.*, 1999). The optimal value of PBIAS is 0. A positive value indicates that the model has underestimated and a negative value indicates overestimation (Gupta *et al.*, 1999). Moriasi *et al.* (2007) suggested that PBIAS is a quick way to quantify water balance errors and indicate model performance. PBIAS is computed with Equation (2).

$$\text{PBIAS} = \frac{\sum_{i=1}^n (Q_{\text{obs}}^i - Q_{\text{sim}}^i) * 100}{\sum_{i=1}^n (Q_{\text{obs}}^i)} \quad (2)$$

The variables in Equation (2) have similar meanings to those in Equation (1).

RESULTS AND DISCUSSION

Model Simulations with Conventional Weather

The model simulation with the conventional weather without calibrations showed a sound performance. The evaluation of the model simulations with observed streamflows at four river gauging stations at a monthly time step yielded reasonable agreement. Using guidelines given in Moriasi *et al.* (2007) for evaluating systematic quantification of watershed simulations at a monthly time step, the NSE results for the Gilgel Abay and Gumera rivers showed *very good* model performance (i.e., $0.75 < \text{NSE} < 1$), while the PBIAS value showed *good* performance ($\pm 10\% < \text{PBIAS} < \pm 15\%$). The NSE and PBIAS values for the Rib and the Megech rivers showed *unsatisfactory* performance ($\text{NSE} \leq 0.50$, and $\text{PBIAS} \geq \pm 25\%$). However, NSE and PBIAS values for the Megech were close to the *satisfactory* model performance criteria (e.g., $\text{NSE} = 0.49$). Table 5 shows the model evaluation statistics for the four river gauging stations.

The hydrograph at a monthly time step showed reasonable agreement between the simulated and the observed streamflows at the four river gauging stations (Figure 3). However, the conventional weather simulation showed minor underestimations for the Gilgel Abay and Gumera and overestimations for the Rib and Megech (Table 5).

In a region with only minor hydro-climatic and biophysical differences, the markedly poor performance of the conventional weather simulation for the Rib river arouses suspicion that there might be weaknesses in the streamflow input data. Ann van Grievsen experienced a similar problem in her research

regarding the Rib River (November 26, 2012, personal communication). However, such a problem has not yet been reported in the literature. This problem was not evident in a study by Setegn *et al.* (2010) of this river basin, but their model evaluation was after calibration, and it is possible to calibrate a model for incorrect data. Overall, we find it highly likely that the performance of the conventional weather simulation for the Rib was compromised by unreliable streamflow input data.

Model Simulations with CFSR Weather

The model simulation using CFSR weather without calibration showed reasonable performance at the Gilgel Abay and Gumera river gauging stations at a monthly time step. The NSE value of more than 0.75

TABLE 5. Model Performance Evaluations for a Monthly Time Step at Four Rivers in the Lake Tana Basin Using Conventional and CFSR Weather Simulations.

Rivers	Conventional Weather		CFSR Weather	
	NSE	PBIAS	NSE	PBIAS
Gilgel Abay	0.87	11.05	0.79	-3.83
Gumera	0.84	9.99	0.75	15.09
Rib	-0.58	-115.69	-0.90	-110.67
Megech	0.49	-29.08	-1.91	-131.88

showed the *very good* performance of the model in these gauging stations. The PBIAS value for Gilgel Abay also indicated *very good* performance, while the PBIAS value for the Gumera showed *good* model performance. The model's performance was *unsatisfactory* for the Rib and Megech rivers, according to both NSE and PBIAS evaluation methods.

The hydrographs and the PBIAS values show that the model simulation with the CFSR weather overestimated the streamflows at three of the four river gauging stations (Figure 4 and Table 5). Comparison of the hydrographs for observed and simulated monthly streamflows at Gilgel Abay showed reasonable agreement, with a minimal overestimation. The simulations at the Gumera gauging station captured most of the peaks, but underestimated a few. The simulation using CFSR weather gave extreme overestimations of streamflow at the Rib and Megech gauging stations. We argued in the previous section that this could well be down to poor data from the Rib gauging station. However, at the Megech station the overestimation was due to high rainfall amount generated by the CFSR weather (Figure 5).

Comparison of the Performance of the Conventional and CFSR Weather Simulations

By Model Evaluation Criteria. According to the model evaluation criteria, the conventional weather simulation performed better than the CFSR

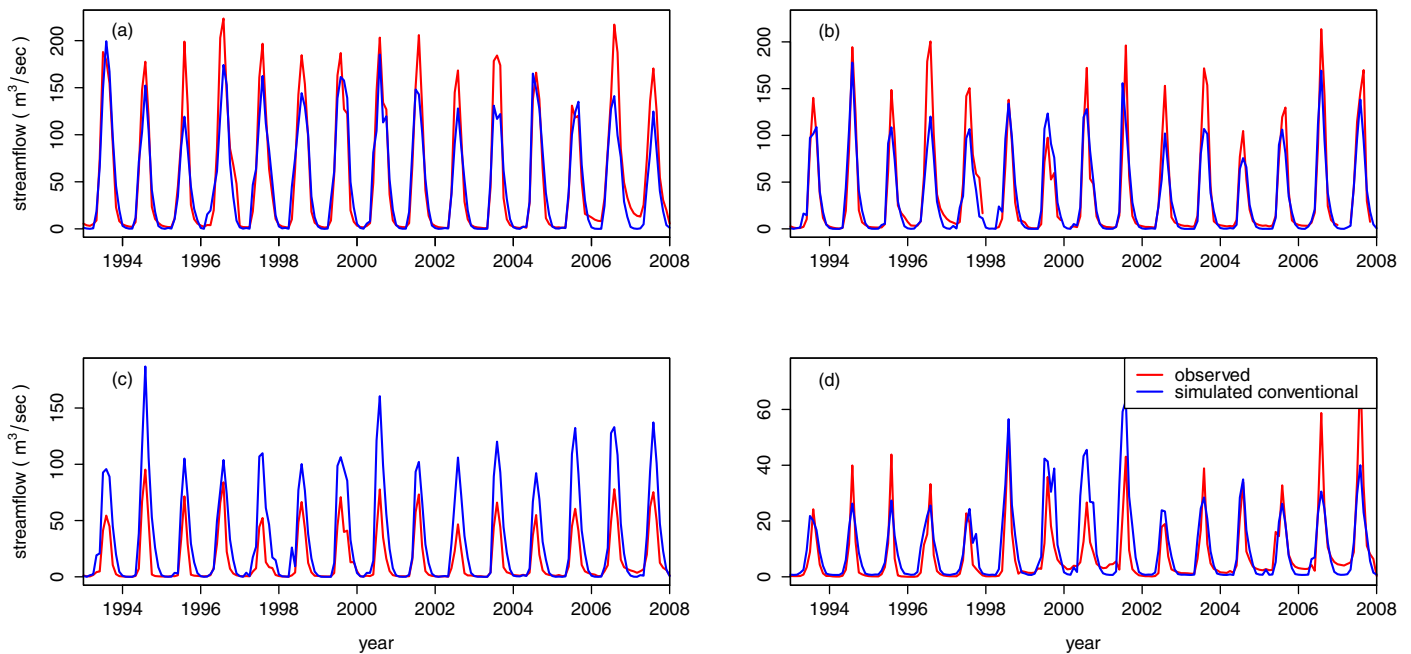


FIGURE 3. Hydrograph between Monthly Observed and Simulated Streamflows with Conventional Weather at (a) Gilgel Abay, (b) Gumera, (c) Rib, and (d) Megech River Gauging Stations During 1993-2007.

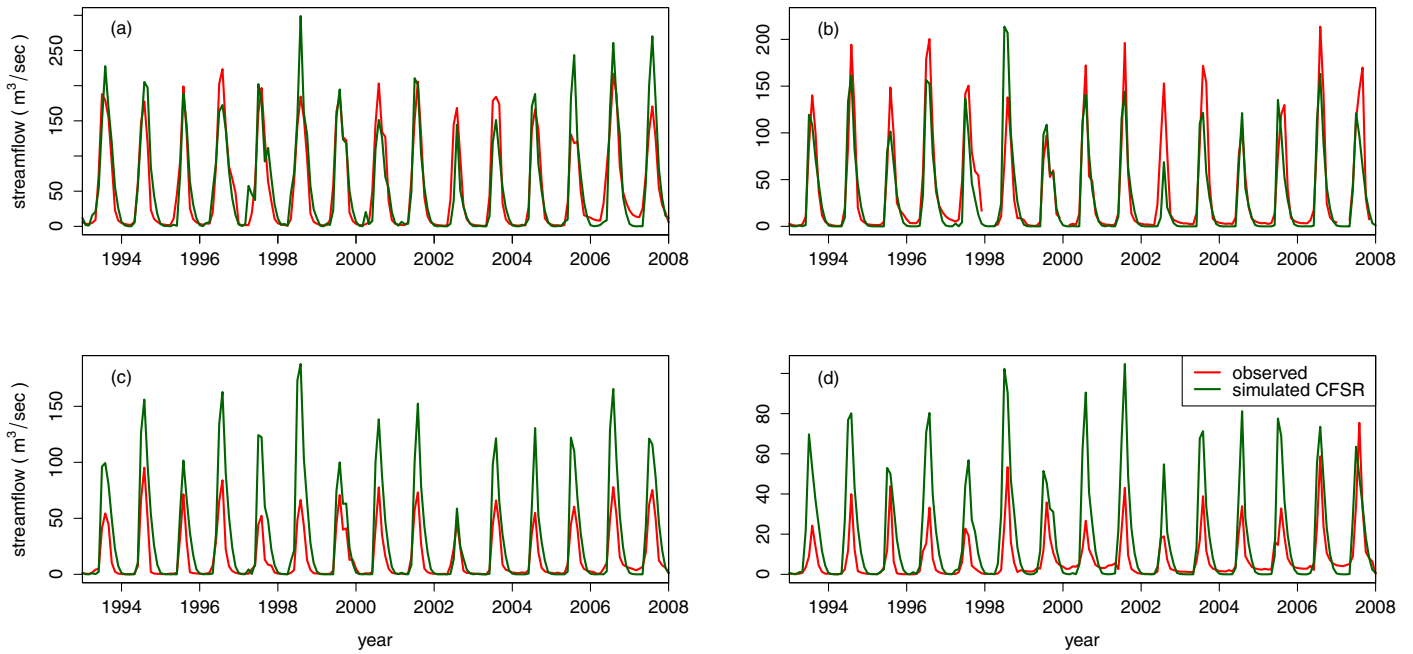


FIGURE 4. Hydrograph between Monthly Observed and Simulated Streamflows with CFSR Weather at (a) Gilgel Abay, (b) Gumera, (c) Rib, and (d) Megech River Gauging Stations.

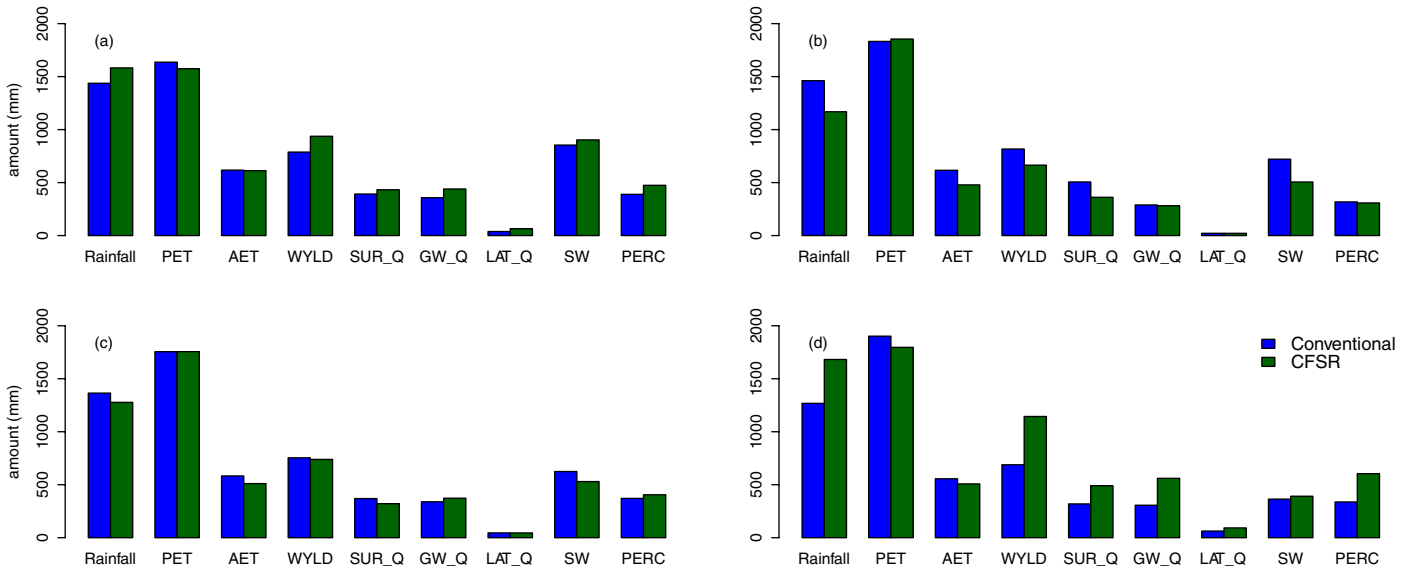


FIGURE 5. Water Balance Components for the Conventional Weather and CFSR Weather Simulations in Four Watersheds of the Lake Tana Basin: (a) Gilgel Abay, (b) Gumera, (c) Rib, and (d) Megech. ET, actual evapotranspiration; WYLD, water yield: the net amount of water that leaves the subbasin and contributes to streamflow in the reach, $WYLD = SUR_Q + LAT_Q + GW_Q - TLOSS$; SUR_Q, surface runoff contribution to streamflow; GW_Q, groundwater contribution to streamflow; LAT_Q, lateral flow contribution to streamflow; SW, soil water content; PERC, water percolating past the root zone; Q-TLOSS, transmission loss.

simulation overall. The model using conventional weather showed at least satisfactory performance for three of the four gauging stations, while the model using CFSR weather showed at least satisfactory performance for two of the gauging stations. Given the uncertainty in the Rib streamflow data, it could be argued that the conventional weather simulation

performed well for all three gauging stations where there was reliable streamflow input data, whereas the CFSR weather simulation performed well for two of them. Regarding the cases where the two weather simulations showed satisfactory performance compared to the observed streamflows, there was no substantial difference.

Simulation of Water Balance Components. Basin-wide water balance partitioning showed that both CFSR and conventional weather generated more or less similar water balance components. The conventional weather simulation converted 43% of the rainfall to streamflow, while the CFSR weather simulation converted 46% to streamflow. However, the contribution of surface runoff and base flow to total streamflow differed in both simulations. The streamflow from the conventional weather simulation had a higher surface runoff contribution (~54%), and the streamflow from the CFSR weather simulation had a higher base flow contribution (~55%). The actual evaporation with the CFSR weather simulation (~75%) was a little higher than the actual evaporation with the conventional weather simulation (~69%). The actual evapotranspiration percentage in the Lake Tana basin was high because of a higher evaporation contribution from the lake. The percolation in the conventional weather simulation was about 20% of rainfall, and 25% in the CFSR weather simulation. Deep percolation in both simulations was 1% of rainfall.

The water balance components from both weather simulations (in each of the four watersheds of the Lake Tana basin) were different (Figure 5). The difference in the water balance components from both weather simulations contributed from the difference in the weather data. The weather data came from two independent sources with different methods for collecting and processing data. A detailed climate data analysis would be needed to investigate the differences between the two weather data (e.g., Silva *et al.*, 2011; Zhang *et al.*, 2012). However, understanding that rainfall is the main factor in hydrological processes, and aiming to demonstrate how the difference in rainfall between the two weather datasets affected the water balance components, we compared the rainfall amounts between the conventional weather and the CFSR weather in the four watersheds.

The average annual rainfall for the CFSR weather over Gilgel Abay and Megech subbasins exceeded the annual rainfall from the conventional weather by 145 and 400 mm respectively. In contrast, the annual rainfall over the Gumera and Rib subbasins from the CFSR weather was less than the average annual rainfall from conventional weather by 290 and 85 mm respectively. The higher rainfall generated by the CFSR weather simulations for the Gilgel Abay and Megech subbasins resulted in higher water balance components (except actual and potential evapotranspiration) than the conventional weather simulations. Conversely, the lower rainfalls in the Gumera and Rib subbasins generated by the CFSR weather simulations resulted in lower values in all water balance

components (except potential evapotranspiration) than the conventional weather simulations.

Simulation of Rainfall. SWAT provides rainfall data at subbasin-by-subbasin level. This allowed us to compare the rainfall amounts from the CFSR and conventional weather for all subbasins in the Lake Tana basin (Figure 6). A large part of the subbasins (~49%) were within a 25% rainfall difference (a conventional rainfall to CFSR rainfall ratio of 0.75-1.0 and 1.0-1.25). Most of the subbasins with a rainfall difference of less than 25% were located further outside the lake boundary. The CFSR weather showed more than 50% rainfall underestimations (a conventional rainfall to CFSR rainfall ratio of more than 1.5) in about 37% of the subbasins, while 14% of the subbasins showed a rainfall difference between 25-50% (a conventional rainfall to CFSR rainfall ratio of 0.5-0.75 and 1.25-1.5). Subbasins with more than 50% rainfall underestimations (with the conventional rainfall to CFSR rainfall ratio of more than 1.5) were located in the lake area and in the southern part of the lake. This indicates that the CFSR weather did not represent rainfall amounts in a large part of the subbasins which are located around Lake Tana.

In much of the gauged part of the Lake Tana basin, the rainfall difference between the CFSR weather and the conventional weather was within 25% (a conventional rainfall to CFSR rainfall ratio of 0.75-1.0 and 1.0-1.25) (Figure 6). In the watersheds of Gilgel Abay, 45% of the subbasins were within a 25% rainfall difference between the CFSR weather and the conventional weather; 28% of the subbasins were within a rainfall difference of 25-50% and the other 27% of the subbasins showed more than 50% rainfall difference. In 80% of the subbasins in Gumera watershed, the rainfall difference between the CFSR weather and the conventional weather were within 25% difference (Figure 6). However, subbasins close to the lake boundary showed very high underestimation where the difference in rainfall between the CFSR weather and the conventional weather was more than 100%. The large part of the subbasins in Rib watershed (~98%) showed a rainfall amount difference between the CFSR and the conventional weather of less than 25%. Around 2% of the subbasins demonstrated more than 25% rainfall difference between the CFSR and conventional weather. In Megech watershed, ~96% of the subbasins showed a rainfall difference between the CFSR and the conventional weather of less than 25%. The remaining 4% showed a difference between 25-50%. Overall, there were underestimations from the CFSR weather in the subbasins of Gumera and Rib, and overestimations in the subbasins of Gilgel Abay and Megech (Figure 6).

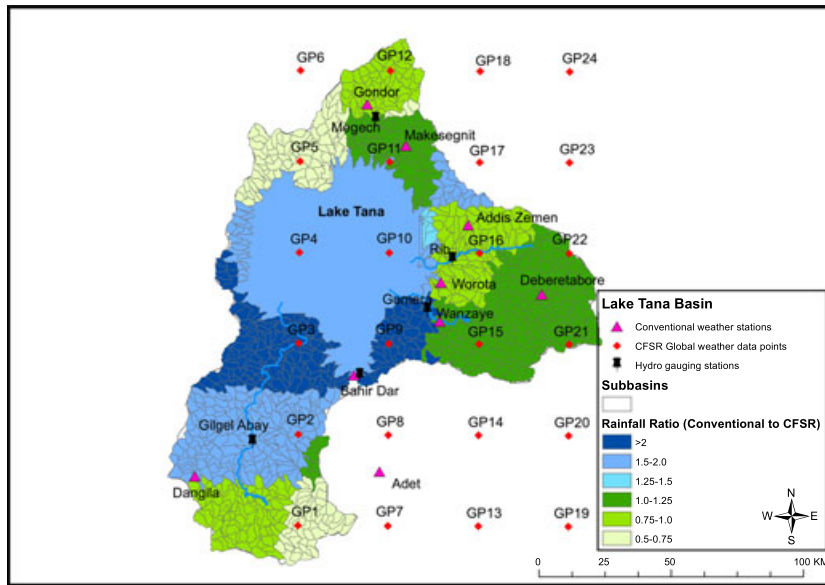


FIGURE 6. Ratio of the Average Annual Rainfall of the Conventional Weather to the Average Annual Rainfall of CFSR Weather. Values greater than 1.0 indicate that the rainfall amount from the conventional weather is higher than the CFSR weather, and vice versa.

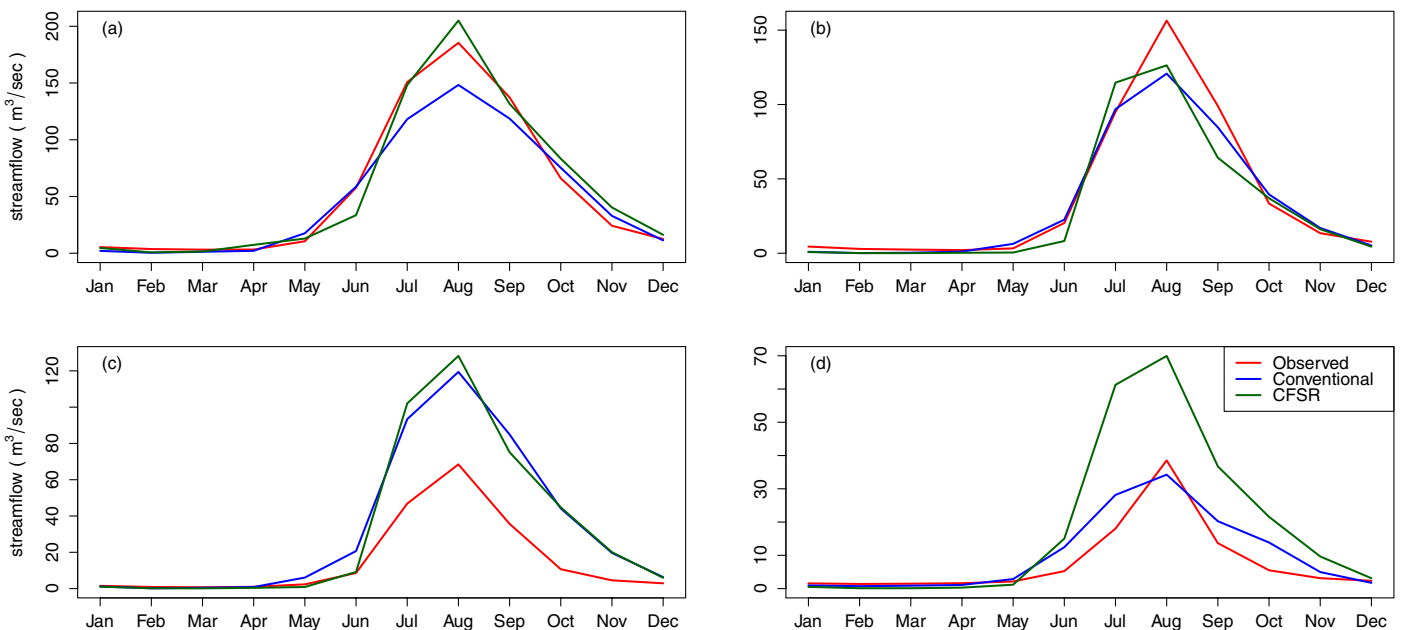


FIGURE 7. Average Monthly Streamflow Hydrograph (1993-2007) for Observed, Simulated with Conventional Weather, and Simulated with CFSR Weather at the (a) Gilgel Abay, (b) Gumera, (c) Rib, and (d) Megech River Gauging Stations in the Lake Tana Basin.

Simulation of Streamflows, Compared with Observed Streamflows. Hydrographs with the long-term average monthly streamflow were used to compare the performance of the conventional and CFSR weather simulations (Figure 7). The CFSR weather simulation replicated the peaks of the observed average monthly streamflows at the Gilgel Abay River gauging station, while the average

monthly streamflow hydrograph generated with conventional weather replicated better the observed low flows and the rising and recession curves (Figure 7a). For the Gumera gauging station, the conventional weather simulation was better at replicating the rising and recession curves of the hydrograph, but both simulations underestimated the peak (Figure 7b). The average monthly hydrographs with the

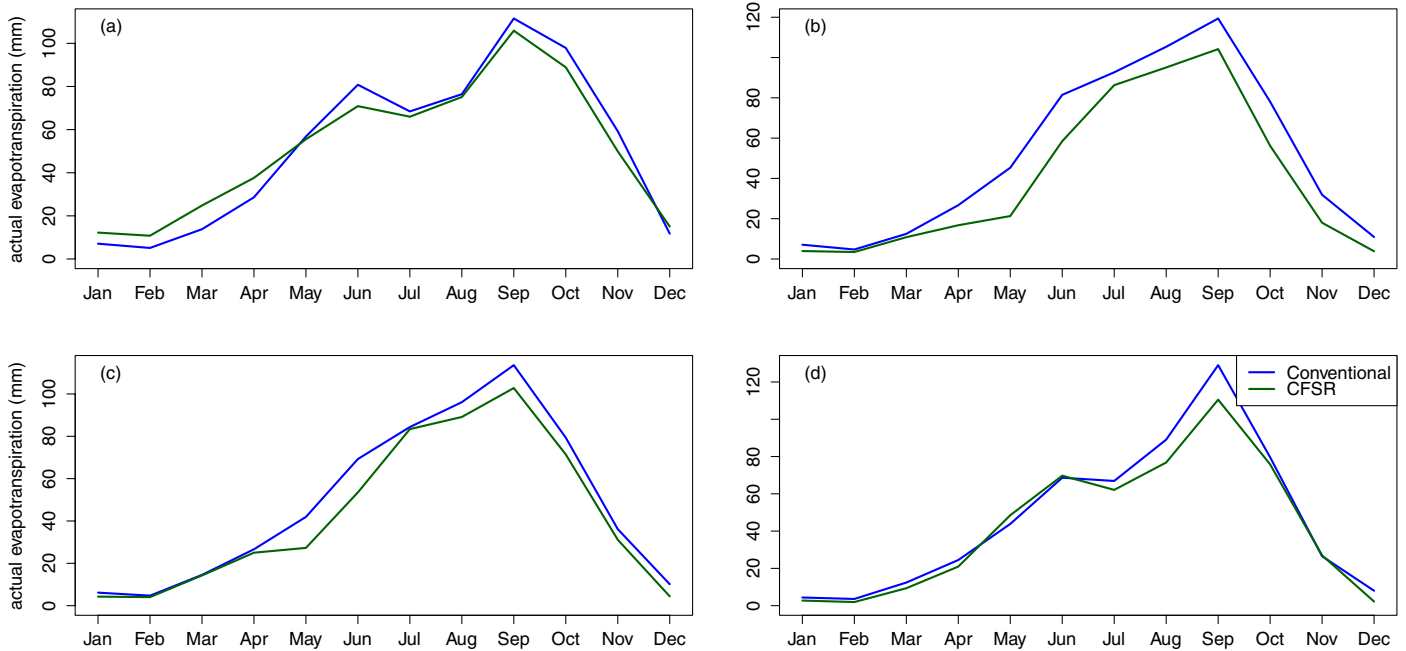


FIGURE 8. Average Monthly Actual Evapotranspiration over the Subbasins of the (a) Gilgel Abay, (b) Gumera, (c) Rib, and (d) Megech Watersheds, Simulated with Conventional Weather and CFSR Weather.

conventional and the CFSR weather at the Rib gauging station behaved similarly except with slight variations during May and June and the peak flow months, but neither replicated the observed streamflows (Figure 7c). The average monthly hydrograph with the CFSR weather simulation overestimated the average monthly observed streamflow at the Megech gauging station (Figure 7d). The average monthly hydrograph with the conventional weather simulation at the Megech gauging station overestimated the rising and the recession limbs of the hydrograph, but underestimated the peak. Overall, the conventional weather simulation performed better at the Megech gauging station than the CFSR weather simulation.

The average monthly streamflows, over 15 years, were lower with the conventional weather simulations for the Gilgel Abay and Megech gauging stations than with the CFSR weather simulations (Table S1, Supporting Information). For the Gumera and Rib rivers, the average monthly streamflows with the conventional weather simulations were higher than with the CFSR weather simulations (Table S1). Figure S1 (Supporting Information) compares the streamflows simulated with the conventional weather and the CFSR weather.

Simulation of Actual Evapotranspiration. We did not have observed actual evapotranspiration data in the Lake Tana basin to compare the performance of the simulations. However, we compared the actual average monthly evapotranspiration from the two simulations to see how the CFSR weather performed

in relation to conventional weather. In most cases, the CFSR weather simulation gave similar or lower estimates than the conventional weather simulation. The only exceptions were in the subbasins of the Gilgel Abay watershed, where the CFSR simulation gave higher average monthly actual evapotranspiration from December to April (Figure 8). The maximum difference between the average monthly actual evapotranspiration simulations in the subbasins of Gilgel Abay was ± 10 mm. The most consistent difference was found in the Gumera subbasins, where the simulation using CFSR weather gave lower average actual evapotranspiration in every month; the maximum deviation (~ 24 mm) occurred in May (Figure 8b). Similarly, the CFSR simulation generated lower average actual evapotranspiration in all months for the Rib subbasins, with the highest difference (~ 16 mm) occurring in June (Figure 8c). The deviation between the average monthly actual evapotranspiration levels generated by the CFSR and conventional weather simulations for the Megech subbasins was less than ± 5 mm in all months except August and September, when it reached 12 and 19 mm respectively (Figure 8d).

Simulation of Crop Yields, Compared with Observed Yields. Crop yields with both weather simulations provided more or less similar results (Figure 9). The simulated average annual teff yield from both weather simulations in all of the four administrative zones was in agreement with the teff yield census data from the CSA (2012), while the corn

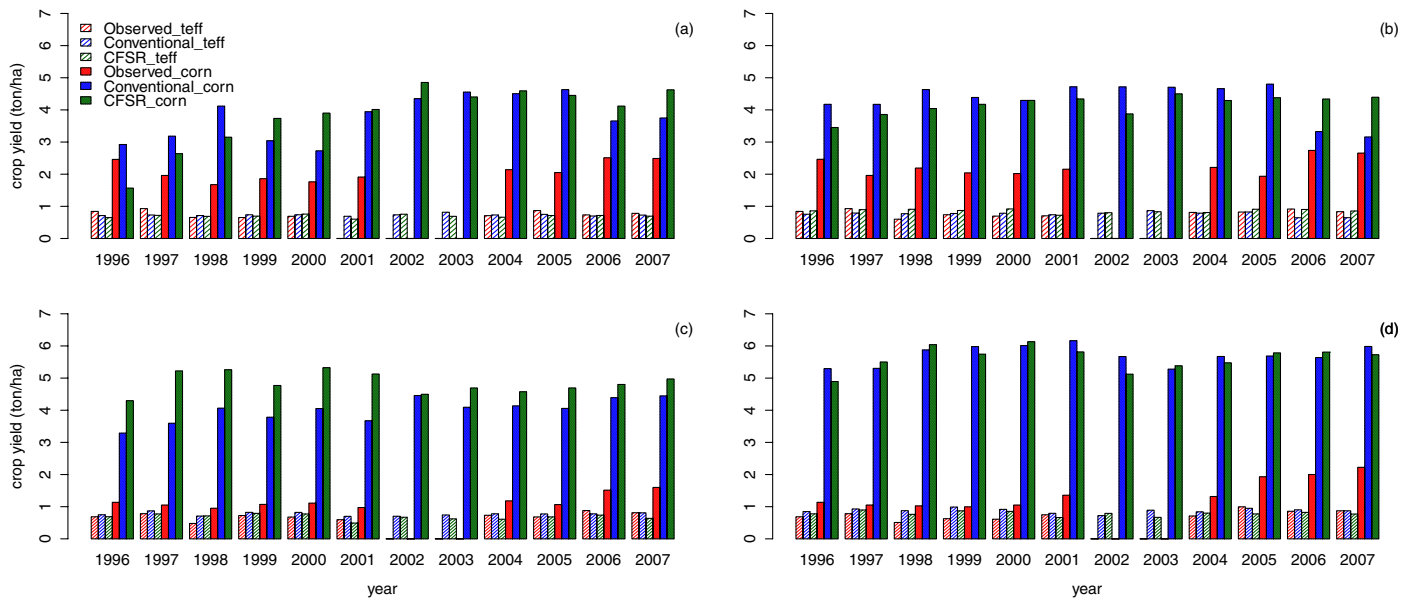


FIGURE 9. Average Annual Crop Yield — Observed (census), Simulated with Conventional Weather, and Simulated with CFSR Weather. (a) Agew Awi, (b) West Gojjam, (c) South Gondor, and (d) North Gondor administrative zones in the Lake Tana basin. Observed data were not available for some years.

yield was overestimated by both weather simulations in all zones. The overestimation was mainly related to higher fertilizer application in cornfields (Figure 2).

As noted above, best-case fertilizer application practice was used in our model. We also checked the effect of high fertilizer application by using lower fertilizer application practices. This showed that adopting lower fertilizer application practices substantially reduced the corn yield. This suggests that the higher corn yield in both weather simulations was related to fertilizer management rather than the weather data per se. We conclude that both weather datasets simulated the crop growth simulation in the Lake Tana basin equally well.

CONCLUSIONS

In this article, we studied the applicability of CFSR weather in predicting the hydrology of the four river basins in the Lake Tana basin, the upper part of the Upper Blue Nile basin of Ethiopia. Our study demonstrated that the CFSR weather simulated the hydrology of the Lake Tana basin with a lower performance rate than conventional weather. CFSR weather gave satisfactory results ($NSE \geq 0.5$) in simulating the observed streamflows at two of the four river gauging stations in the basin, while the conventional weather provided satisfactory results at three of the stations. Simulation with the conventional

weather substantially underestimated streamflow (PBIAS of -116%) only at the Rib gauging station, where the authors and other researchers (e.g., Ann van Grievsen, UNESCO-IHE, November 26, 2012, personal communication) suspect input data problems. However, simulation with CFSR weather substantially underestimated streamflow at both Rib and Megech stations (PBIAS of -111 and -132% , respectively).

The water balance components from the two simulations were not significantly different, except for the Megech watershed. The average annual rainfall from CFSR weather over the Gilgel Abay and Megech subbasins was higher than the annual rainfall from the conventional weather by 145 and 400 mm, respectively. The water balance components were thus higher in the CFSR weather simulations than the conventional weather simulations at both watersheds. While the overestimation for Gilgel Abay was relatively small, for Megech it was substantial. The annual rainfall over the Gumera and Rib subbasins from the CFSR weather was lower than the average annual rainfall from conventional weather by 290 and 85 mm, respectively. The lower rainfall in the CFSR weather was reflected in generally lower water balance component values in the CFSR weather simulations. Overall, the difference in the water balance components from the simulations using both sets of weather data was minor in three of the four watersheds.

Both weather datasets provided similar crop yield simulations. Both simulations estimated teff yields close to those observed by the Ethiopian Central

Statistical Agency (CSA, 2012) in all four administrative zones in the Lake Tana basin, while corn yields were overestimated in all four zones compared to the observed data. The higher corn yields in both weather simulations were associated with high fertilizer application in the model.

These results indicate that while CFSR weather is no substitute for high-quality observed weather, it may be useful where such data are lacking. It is not always easy to find conventional weather stations at a given spatial and temporal resolution, especially in developing countries. Moreover, when the data exist, they may be unreliable because of gaps and other problems, such as random errors. In such cases, it may be better to use global data sources such as CFSR. CFSR weather has an advantage over conventional weather in that it provides complete sets of climatic data. This allows the flexibility to apply different functions pertaining to hydrological models. For example, with the conventional weather, we were limited to using the Hargreaves method to calculate potential evapotranspiration because this method only requires maximum and minimum temperatures to calculate potential evapotranspiration. However, availability of wind speed, relative humidity, and solar radiation data in the CFSR weather provides the flexibility to use Penman-Montieth and Priestley-Taylor methods. All in all, while hydrological model simulations should use high-quality observed weather data when available, CFSR weather is a viable option for simulating the hydrology of an area in data-scarce regions.

SUPPORTING INFORMATION

Additional Supporting Information may be found in the online version of this article:

Table S1. Mean Monthly Streamflows (over 15 year's period) at Gilgel Abay, Gumera, Rib, and Megech River Gauging Stations with Conventional Weather and CFSR Weather Simulations.

Figure S1. Hydrographs for Monthly Stream Flows with the Conventional Weather and CFSR Weather Simulations at the (a) Gilgel Abay, (b) Gumera, (c) Rib, and (d) Megech River Gauging Stations.

ACKNOWLEDGMENTS

The first author is sponsored by the Swedish Research Council for Environment, Agricultural Sciences and Spatial Planning (Formas) and Stockholm Environment Institute (SEI). He was a short-term exchange scholar at the Spatial Sciences Laboratory at the Department of Ecosystem Sciences and Management at Texas

A&M University when this paper was submitted. The authors would like to express their appreciation to Louise Karlberg of SEI for her invaluable comments. Comments from four anonymous reviewers were also extremely helpful in improving the manuscript.

LITERATURE CITED

- Abdo, K.S., B.M. Fiseha, T.H.M. Rientjes, A.S.M. Gieske, and A.T. Haile, 2009. Assessment of Climate Change Impacts on the Hydrology of Gilgel Abay Catchment in Lake Tana Basin, Ethiopia. *Hydrological Processes* 23:3661-3669.
- Andersson, J.C.M., A.J.B. Zehnder, B. Wehrli, and H. Yang, 2012. Improved SWAT Model Performance with Time-Dynamic Voronoi Tessellation of Climatic Input Data in Southern Africa. *Journal of the American Water Resources Association* 48:480-493.
- Barrett, C.B., 1994. The Development of the Nile Hydrometeorological Forecast System. *Water Resources Bulletin* 29:933-938.
- Betrie, G.D., Y.A. Mohamed, A. van Griensven, and R. Srinivasan, 2011. Sediment Management Modelling in the Blue Nile Basin Using SWAT Model. *Hydrology and Earth System Sciences* 15:807-818.
- Beyene, T., D.P. Lettenmaier, and P. Kabat, 2009. Hydrologic Impacts of Climate Change on the Nile River Basin: Implications of the 2007 IPCC Scenarios. *Climatic Change* 100:433-461.
- CGIAR-CSI, 2009. SRTM 90m Digital Elevation Data. <http://srtm.csi.cgiar.org/>, accessed February 2009.
- Collick, A.S., Z.M. Easton, T. Ashagrie, B. Biruk, S. Tilahun, E. Adgo, S.B. Awulachew, G. Zeleke, and T.S. Steenhuis, 2009. A Simple Semi-Distributed Water Balance Model for the Ethiopian Highlands. *Hydrological Processes* 23:3718-3727.
- Conway, D., 2009. A Water Balance Model of the Upper Blue Nile in Ethiopia. *Hydrological Sciences Journal* 42:265-286.
- Conway, D. and H. Mike, 1996. The Impacts of Climate Variability and Future Climate Change in the Nile Basin on Water Resources in Egypt. *International Journal of Water Resources Development* 12:277-296.
- Conway, D. and E.L. Schipper, 2011. Adaptation to Climate Change in Africa: Challenges and Opportunities Identified from Ethiopia. *Global Environmental Change* 21:227-237.
- CSA, 2012. Central Statistical Authority of Ethiopia. <http://www.csa.gov.et/>.
- Easton, Z.M., D. Fuka, E. White, A.S. Collick, B.B. Ashagre, M. McCartney, and S. Awulachew, 2010. A Multi Basin SWAT Model Analysis of Runoff and Sedimentation in the Blue Nile, Ethiopia. *Hydrology and Earth System Sciences* 14:1827-1841.
- EIAR, 2007. Crop Technologies Usage. Ethiopian Institute of Agricultural Research, Addis Ababa, Ethiopia (in Amharic).
- Elshamy, M.E., I.A. Seierstad, and A. Sorteberg, 2009. Impacts of Climate Change on Blue Nile Flows Using Bias-Corrected GCM Scenarios. *Hydrology and Earth System Sciences* 13:551-565.
- Engida, A.N. and M. Esteves, 2011. Characterization and Disaggregation of Daily Rainfall in the Upper Blue Nile Basin in Ethiopia. *Journal of Hydrology* 399:226-234.
- ENMSA, 2012. Metreological Data. The Ethiopian National Metreological Services Agency, Addis Ababa, Ethiopia.
- FAO, 1995. World Soil Resources: An Explanatory Note on the FAO (Food and Agriculture Organization) World Soil Resources Map at 1:25 000 00 Scale. Food and Agriculture Organization of the United Nations, Rome, Italy.
- Fuka, D.R., M.T. Walter, C. MacAlister, A.T. Degaetano, T.S. Steenhuis, and Z.M. Easton, 2013. Using the Climate Forecast

- System Reanalysis as Weather Input Data for Watershed Models. *Hydrological Processes*, doi: 10.1002/hyp.10073.
- Gebregziabher, S., A.M. Mouazen, H. Van Brussel, H. Ramon, J. Nyssen, H. Verplancke, M. Behailu, J. Deckers, and J. de Baerdemaeker, 2006. Animal Drawn Tillage, the Ethiopian Arid Plough, Maresha: A Review. *Soil and Tillage Research* 89:129-143.
- Gebrehiwot, S.G., U. Ilstedt, A. I. Gärdenas, and K. Bishop, 2011. Hydrological Characterization of Watersheds in the Blue Nile Basin, Ethiopia. *Hydrology and Earth System Sciences* 15:11-20.
- Globalweather, 2012. NCEP Climate Forecast System Reanalysis (CFRS). <http://globalweather.tamu.edu/>, accessed December 2012.
- Gupta, H., S. Sorooshian, and P. Yapo, 1999. Status of Automatic Calibration for Hydrologic Models: Comparison with Multilevel Expert Calibration. *Journal of Hydrologic Engineering* 4:135-143.
- GWSA, 2012. Angereb Reservoir Data. Gondor Town Municipality Water Supply Authority, Gondor, Ethiopia.
- Kim, U. and J. Kaluarachchi, 2008. Application of Parameter Estimation and Regionalization Methodologies to Ungauged Basins of the Upper Blue Nile River Basin, Ethiopia. *Journal of Hydrology* 362:39-56.
- Kim, U. and J.J. Kaluarachchi, 2009. Climate Change Impacts on Water Resources in the Upper Blue Nile River Basin, Ethiopia. *Journal of the American Water Resources Association* 45:1361-1378.
- Kim, U., J.J. Kaluarachchi, and V.U. Smakhtin, 2008. Generation of Monthly Precipitation Under Climate Change for the Upper Blue Nile River Basin, Ethiopia. *Journal of the American Water Resources Association* 44:1231-1247.
- Lavers, D.A., G. Villarini, R.P. Allan, E.F. Wood, and A.J. Wade, 2012. The Detection of Atmospheric Rivers in Atmospheric Reanalyses and Their Links to British Winter Floods and the Large-Scale Climatic Circulation. *Journal of Geophysical Research* 117:D20106.
- Liu, B.M., A.S. Collick, G. Zeleke, E. Adgo, Z.M. Easton, and T.S. Steenhuis, 2008. Rainfall-Discharge Relationships for a Monsoonal Climate in the Ethiopian Highlands. *Hydrological Processes* 22:1059-1067.
- Mekonnen, M.A., A. Wörman, B. Dargahi, and A. Gebeyehu, 2009. Hydrological Modelling of Ethiopian Catchments Using Limited Data. *Hydrological Processes* 3408:3401-3408.
- Melesse, A., W. Abtew, T. Dessalegne, and X. Wang, 2010. Low and High Flow Analyses and Wavelet Application for Characterization of the Blue Nile River System. *Hydrological Processes* 252:241-252.
- Mishra, A. and T. Hata, 2006. A Grid-Based Runoff Generation and Flow Routing Model for the Upper Blue Nile Basin. *Hydrological Sciences Journal* 51:191-206.
- Mohamed, Y., B. van den Hurk, H. Savenije, and W. Bastiaanssen, 2005. Hydroclimatology of the Nile: Results from a Regional Climate Model. *Hydrology and Earth System Sciences* 9:263-278.
- Moriasi, D.N., J.G. Arnold, M.W. van Liew, R.L. Bingner, R.D. Harmel, and T.L. Veith, 2007. Model Evaluation Guidelines for Systematic Quantification of Accuracy in Watershed Simulations. *Transactions of the ASABE* 50:885-900.
- MoWE, 2012. Hydrological Data. The Ethiopian Ministry of Water and Energy (MoWE), Addis Ababa, Ethiopia.
- MoWR, 1998. Abay River Basin Integrated Development Master Plan Project. Ethiopia Ministry of Water Resources, Addis Ababa, Ethiopia, 140 pp.
- MoWR, 2009. Spatial Data. The Ethiopian Ministry of Water Resources, Addis Ababa, Ethiopia.
- Najafi, M.R., H. Moradkhani, and T.C. Piechota, 2012. Ensemble Streamflow Prediction: Climate Signal Weighting Methods vs. Climate Forecast System Reanalysis. *Journal of Hydrology* 442-443:105-116.
- Nash, J.E. and J.V. Sutcliffe, 1970. River Flow Forecasting through Conceptual Models: Part 1. — A Discussion of Principles. *Journal of Hydrology* 10:282-290.
- Neitsch, S.L., J.G. Arnold, J.R. Kiniry, and J. R. Williams, 2012. Soil and Water Assessment Tool Theoretical Documentation: Version 2005. Grassland Soil and Water Research Laboratory, Agricultural Research Service, Blackland Research Center, Texas Agricultural Experiment Station, Temple, Texas.
- Quadro, M.F.L., E.H. Berbery, M.A.F. Silva Dias, D.L. Herdies, and L.G.G. Gonçalves, 2013. The Atmospheric Water Cycle over South America as Seen in the New Generation of Global Reanalyses. *AIP Conference Proceedings* 732:732-735.
- Saha, S., S. Moorthi, H.-L. Pan, X. Wu, J. Wang, S. Nadiga, P. Tripp, R. Kistler, J. Woollen, D. Behringer, H. Liu, D. Stokes, R. Grumbine, G. Gayno, J. Wang, Y.-T. Hou, H.-Y. Chuang, H.-M.H. Juang, J. Sela, M. Iredell, R. Treadon, D. Kleist, P. Van Delst, D. Keyser, J. Derber, M. Ek, J. Meng, H. Wei, R. Yang, S. Lord, H. Van Den Dool, A. Kumar, W. Wang, C. Long, M. Chelliah, Y. Xue, B. Huang, J.-K. Schemm, W. Ebisuzaki, R. Lin, P. Xie, M. Chen, S. Zhou, W. Higgins, C.-Z. Zou, Q. Liu, Y. Chen, Y. Han, L. Cucurull, R.W. Reynolds, G. Rutledge, and M. Goldberg, 2010. The NCEP Climate Forecast System Reanalysis. *Bulletin American Meteorological Society* 91:1015-1057.
- Setegn, S.G., D. Rayner, A.M. Melesse, B. Dargahi, and R. Srinivasan, 2011. Impact of Climate Change on the Hydroclimatology of Lake Tana Basin, Ethiopia. *Water Resources Research* 47: W04511.
- Setegn, S.G., R. Srinivasan, A.M. Melesse, and B. Dargahi, 2010. SWAT Model Application and Prediction Uncertainty Analysis in the Lake Tana Basin, Ethiopia. *Hydrological Processes* 367:357-367.
- Silva, V.B.S., V.E. Kousky, and R.W. Higgins, 2011. Daily Precipitation Statistics for South America: An Intercomparison Between NCEP Reanalyses and Observations. *Journal of Hydrometeorology* 12:101-117.
- Smith, R.A. and C.D. Kummerow, 2013. A Comparison of *in situ*, Reanalysis, and Satellite Water Budgets over the Upper Colorado River Basin. *Journal of Hydrometeorology* 14:888-905.
- Taye, M., V. Ntegeka, and P. Willems, 2011. Assessment of Climate Change Impact on Hydrological Extremes in Two Source Regions of the Nile River Basin. *Hydrology and Earth System Sciences* 15:209-222.
- Temesgen, M., J. Rockstrom, H.H.G. Savenije, W.B. Hoogmoed, and D. Alemu, 2008. Determinants of Tillage Frequency Among Smallholder Farmers in Two Semi-Arid Areas in Ethiopia. *Physics and Chemistry of the Earth, Parts A/B/C* 33:183-191.
- Tesemma, Z.K., Y.A. Mohamed, and T.S. Steenhuis, 2009. Trends in Rainfall and Runoff in the Blue Nile Basin: 1964-2003. *Hydrological Processes* 24:3747-3758.
- Tsintikidis, D., K.P. Georgakakos, G.A. Artan, and A.A. Tsonis, 1999. A Feasibility Study on Mean Areal Rainfall Estimation and Hydrologic Response in the Blue Nile Region Using METEOSAT Images. *Journal of Hydrology* 221:97-116.
- Uhlenbrook, S., Y. Mohamed, and A.S. Gragne, 2010. Analyzing Catchment Behavior through Catchment Modeling in the Gilgel Abay, Upper Blue Nile River Basin, Ethiopia. *Hydrology and Earth System Sciences* 14:2153-2165.
- Wale, A., T.H.M. Rientjes, A.S.M. Gieske, and H.A. Getachew, 2009. Ungauged Catchment Contributions to Lake Tana's Water Balance. *Hydrological Processes* 23(26):3682-3693.
- Wei, W., C. Jilong, and H. Ronghui, 2013. Water Budgets of Tropical Cyclones: Three Case Studies. *Advances in Atmospheric Sciences* 30:468-484.
- White, E.D., Z.M. Easton, D.R. Fuka, A.S. Collick, E. Adgo, M. McCartney, S.B. Awulachew, Y.G. Selassie, and T.S. Steenhuis,

2011. Development and Application of a Physically Based Landscape Water Balance in the SWAT Model. *Hydrological Processes* 25:915-925.
- Ymeti, I., 2007. Rainfall Estimation by Remote Sensing for Conceptual Rainfall-Runoff Modeling in the Upper Blue Nile Basin. Rainfall Estimation by Remote Sensing for Conceptual Rainfall-Runoff Modeling in the Upper Blue Nile Basin. MSc. Thesis, International Institute for Geo-Information Science and Earth Observation, Enschede, The Netherlands.
- Zhang, Q., H. Körnich, and K. Holmgren, 2012. How Well Do Reanalyses Represent the Southern African Precipitation? *Climate Dynamics*, doi: 10.1007/s00382-012-1423-z.